Numerical simulations of Typhoon Rai (2021) by two nonhydrostatic atmosphere models and an atmosphere-wave ocean coupled model

Akiyoshi Wada, Wataru Yanase, and Satoki Tsujino

Meteorological Research Institute, Tsukuba, Ibaraki, 305-0052, JAPAN

[1]awada@mri-jma.go.jp

1. Introduction

A tropical depression developed to a tropical storm (named Rai) around (6.0˚N, 141.0˚E) at 06 UTC on 13 December 2021. Rai moved west-northwestward in the intensification phase and then made landfall in the Philippines. Rai reached the minimum central pressure of 915 hPa at 06 UTC on 16 December over the Philippines Sea and at 18 UTC on 18 December after the TC moved into the South China Sea. The double peaks with a central pressure of 915 hPa have never been observed in TCs in December before.

To investigate the possibility of the prediction of the record-breaking double peaks, numerical simulations were conducted for Rai by using an operational nonhydrostatic atmosphere model (asuca: Asuca is a System based on a Unified Concept for Atmosphere), a nonhydrostatic atmosphere model (NHM, Wada et al., 2018) and the coupled atmosphere-wave-ocean model (CPL, Wada et al., 2018).

2. Experimental design

Table 1 shows a list of numerical simulations. Each initial time was 0000 UTC on 13 December 2021. The computational domain was 5000 x 2000 km with a grid spacing of 2 km (Fig. 1a). The number of the vertical layer was 55 for NHM and CPL and 96 for the asuca. The top height was approximately 27 km for NHM and CPL and approximately 37 km for asuca. The integration time in all simulations was 156 hours.

Table1 List of numerical simulations

Name	*Model*	*IRE*	*Cumulus Parameterization*
NHM	NHM	0.2	None
CPL	CPL	0.2	None
asuca (1.0)	asuca	1.0	KF: Kain and Fritsch (1990)
asuca (0.0)	asuca	0.0	KF: Kain and Fritsch (1990)

The time step was 5 seconds for the NHM, the asuca, and the atmospheric part of CPL, 30 seconds for the ocean model incorporated into the CPL, and 6 minutes for the ocean surface wave model incorporated into the CPL. The cumulus parameterization of Kain and Fritsch (1990) (KF in Table 1) was used only for the asuca. The setting of KF was the same as that in the local forecast model operationally used in JMA. The atmospheric boundary-layer scheme used in the NHM and CPL was the same as that in Wada et al. (2018), while Mellor-Yamada-Nakanishi-Niino level 2.5 closure scheme (e.g. Nakanishi and Niino, 2009) was used in the numerical simulations conducted by the asuca. The inhibition rate of evaporation (IRE) of rain, snow, and graupel included in the cloud physics for the NHM and CPL was 0.2, while three sensitivity experiments were conducted by the asuca on the IRE by using the following two values (1.0, 0.0).

The JMA global objective analysis with the horizontal resolution of 20 km and the JMA North Pacific Ocean analysis with the horizontal resolution of 0.5° were used for creating atmospheric and oceanic initial conditions and atmospheric lateral boundary conditions. As for the initial condition of sea surface temperature (SST), the Optimally Interpolated SST (OISST) daily product with the horizontal resolution of 0.25°, obtained from the Remote Sensing Systems (http://www.remss.com) was used. The Regional Specialized Meteorological Center (RSMC) Tokyo best track data (https://www.jma.go.jp/jma/jma-eng/jma-center/rsmc-hp-pub-eg/besttrack.html) was used to validate the results of numerical simulations.

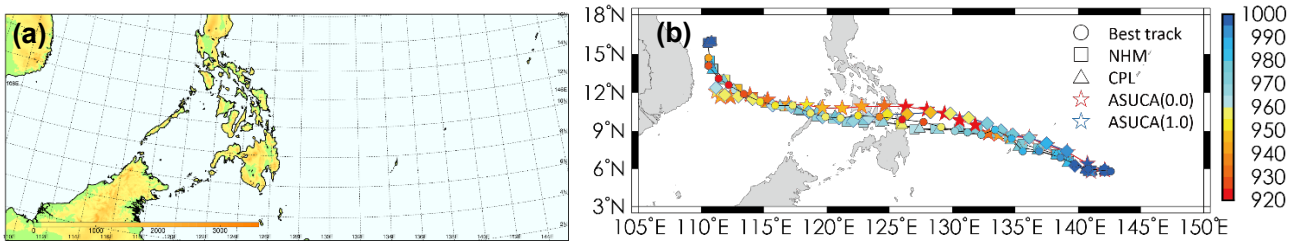

Figure 1 (a) Computational domain. (b) Track simulation results with the RSMC best track. Colors in the marks and vertical bar indicate the value of central pressure (hPa).

3. Results

3.1 Tracks

Figure 1b shows that the tracks in all simulations are in good agreement with the RSMC Tokyo best track data. The tracks simulated by the asuca show a northward deflection compared to the best track before and during making landfall in the Philippines. After the landfall, all simulated tracks show that the moving direction was westward to west-northwestward and then changed to the northward direction at around (12˚N, 112.0˚E). Around the recurvature

area in the South China Sea, the track of simulated Rai shows a slightly southwestward deflection compared to the best track.

3.2 Intensity changes

Figure 2 shows the time series of simulated central pressure with the best-track central pressure from 00 UTC on 13 December to 12 UTC on 19 December. The simulated central pressure in the experiment asuca (0.0) decreased more rapidly than that in the experiment asuca (1.0). Compared to the results simulated by the asuca, the results simulated by the NHM and CPL show a relatively high value of the minimum central pressures, but the timing of the first peak of simulated minimum central pressure is consistent with that in the best track data.

Around the recurvature area in the South China Sea, the timeseries of minimum central pressure in the RSMC best track data indicates the occurrence of the second peak intensity. The simulated central pressures in the South China Sea was relatively high at the timing compared to the RSMC best track intensity.

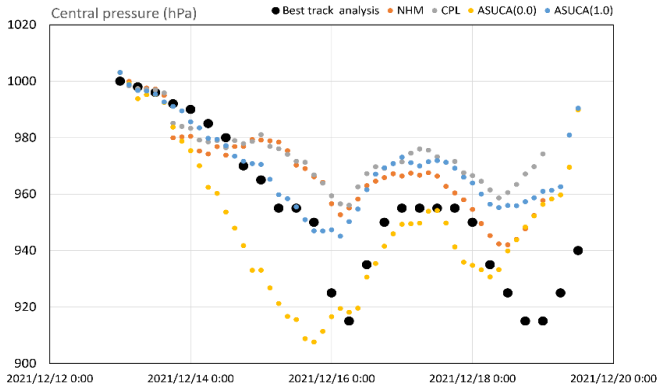

Figure 2 Time series of simulated central pressures with the best-track central pressure (hPa).

The impact of ocean coupling on simulated central pressures represented by the difference between the NHM and CPL was distinct at the second peak. Without the ocean coupling, the central pressure simulated by the NHM was the lowest in the South China Sea, while the other simulation showed that the simulated central pressure was the lowest east of the Philippines.

3.3 Rainfall structure

Figure 3 shows the horizontal distributions of simulated hourly rainfall and 89GHz Polarized Corrected Temperature (PCT). The size of the storm's eye simulated by the NHM and CPL was relatively large compared with the eye observed in Fig. 3e. The horizontal distributions of hourly rainfall simulated by the NHM (Fig. 3a) and CPL (Fig. 3b) show an axisymmetric pattern. The east-west spreading simulated rainband on the north side corresponded to that in the satellite analysis (Fig .3e) although the distribution simulated by the NHM differed from that simulated by the CPL. The horizontal distribution in the experiment asuca (0.0) (Fig. 3c) shows an asymmetric pattern with smaller eye than in the NHM and CPL simulations (Figs. 3a, b). However, the size of the storm's eye became large when the IRE was 1.0 (Fig. 3d) since the simulated central pressure in the experiment asuca (1.0) was much higher than that in the experiment asuca (0.0) (Fig. 2).

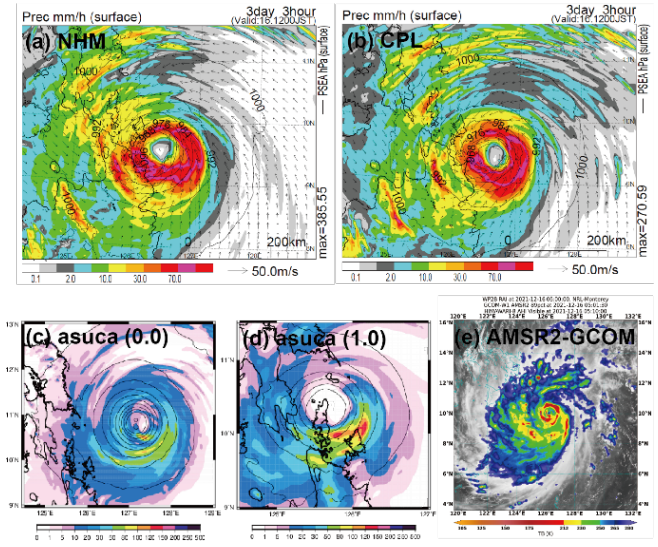

Figure 3 Horizontal distributions of hourly rainfall at 03 UTC on 16 December in 2021 simulated by the (a) NHM, (b) CPL, and (c-d) asuca (see Table 1 for the difference in the IRE). (e) 89GHz PCT at around 05 UTC on 16 December.

4. Concluding remarks

The simulation results successfully reproduced the storm's track and double intensity peaks. However, all models could not quantitatively predict the intensity particularly the peak intensity in the South China Sea. Although the first intensity peak of Rai east of the Philippines was simulated better than the second intensity peak in the South China Sea in the experiment asuca (0.0), the inner-core structure such as the small eye size of the storm and fine eyewall structure before making landfall in the Philippines could not be simulated realistically. The lack of fine inner-core structure of simulated Rai may be the reason why the rapid intensification could not be predicted at all in the first intensity peak and subsequently in the second intensity peak.

References

Kain, J. S., and J. M. Fritsch (1990). A one-dimensional entraining/detraining plume model and its application in convective parameterization. Journal of the Atmospheric Sciences, 47, 2784-2802.

Nakanishi, M., and H. Niino (2009). Development of an improved turbulence closure model for the atmospheric boundary layer. Journal of the Meteorological Society of Japan, 87, 895-912.

Wada, A., S. Kanada, and H. Yamada (2018). Effect of air–sea environmental conditions and interfacial processes on extremely intense typhoon Haiyan (2013). Journal of Geophysical Research: Atmospheres, 123, 10379-10405.